

BRANCH-BASED REGION GROWING METHOD FOR BLOOD VESSEL SEGMENTATION

S.Eiho^a, H.Sekiguchi^a, N.Sugimoto^a, T.Hanakawa^b, S.Urayama^b

^a Graduate School of Informatics, Kyoto University, Gokasho, Uji-shi, 611-0011 Japan –
eiho@image.kuass.kyoto-u.ac.jp

^b Human Brain Research Center, Graduate School of Medicine, Kyoto University, Shogoin Sakyo-ku, Kyoto-shi,
606-8507 Japan

KEY WORDS: Segmentation, MRA, MIP, Blood Vessel, Region Growing

ABSTRACT:

We propose an algorithm of blood vessel segmentation for MRA data in this paper. The generic region growing, as well as thresholding, is not appropriate to extract the whole part of the vessels on MRA data. This is because of the image property of the MRA, where the intensity of each pixel on the blood area depends on the amount of blood flow. Moreover, thin vessels are affected by the partial volume effect which reduces the intensity of vessel parts as the low pass filtering effect. So the range of the intensity of the blood vessel in MRA image is not restricted in a small interval but spread widely. To get correct segmentation results by region growing, the growing condition should be flexibly adapted according to the local characteristics in each ROI. We have designed a branch-based region growing for this purpose. Since its growing process is performed on one branch at a time, the growing conditions can be optimized according to its surrounding properties. It is also possible to connect a break point by extending the vessel, which improves segmentation results. By applying this method to 5 head MRA data sets, the availability of the method has been confirmed. In addition, to evaluate the segmentation result quantitatively, we developed a new evaluation method which utilizes MIP data.

1. INTRODUCTION

MRA (magnetic resonance angiography) and CTA (X-ray CT angiography) are widely used for the diagnosis of serious circulation diseases. These data are basically slice images, and it is difficult to understand vessel's shape and their perspective locations on the slice data. This is the reason why MIP (maximum intensity projection) or 3-D image is used for diagnosis. These images are created by accumulating a lot of MRA/CTA slice images.

Figure 1 shows an example of MIP and 3-D image. Both images are created from the same MRA data, but features and image quality of them are quite different. In general, 3-D image is superior to MIP in regard to both reality and perspective.

In recent years, 3-D images are commonly used for CTA diagnosis and a lot of 3-D applications have been developed. On the contrary, MIP is mainly used for MRA diagnosis.

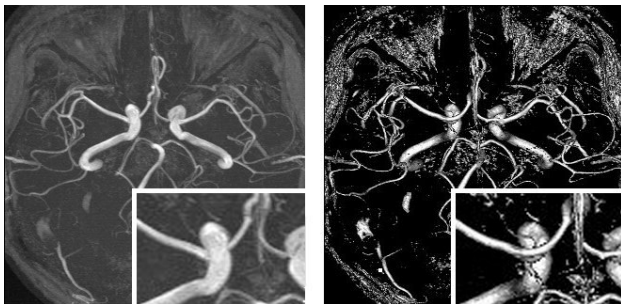


Figure 1. Comparison of MIP (left) and 3-D image (right).

The reasons why 3-D images are not used for MRA data are:

1. Creating 3-D image requires blood vessel segmentation.
2. Blood vessel segmentation on MRA data is quite difficult.

If blood vessel segmentation is easily obtainable, 3-D image will be available on MRA diagnosis. MRA is the only imaging method of blood circulation without invasiveness, and so, it is strongly desired to realize the blood vessel segmentation for MRA data.

2. METHODS

2.1 Problems in the conventional methods

As the range of the blood vessel intensity in MRA is widely spread, conventional binarizing method is unable to extract blood vessel region. The same is true for region growing, because the growing condition is also determined from the range of the intensity value. In addition, when the growing proceeds in the narrow and long vessels, it often stops the growing on the way because of noise or insufficient resolution of the image.

To overcome this problem, it is obvious that the growing condition has to be changed adaptively according to the local vessel intensity. But a conventional region growing has several growing points simultaneously as shown in Figure 2, and it can hold one growing condition at a time. To solve the problem, we proposed a new kind of region growing which keeps spreading in restriction along only one vessel. Hereinafter we call it “branch-based region growing”.

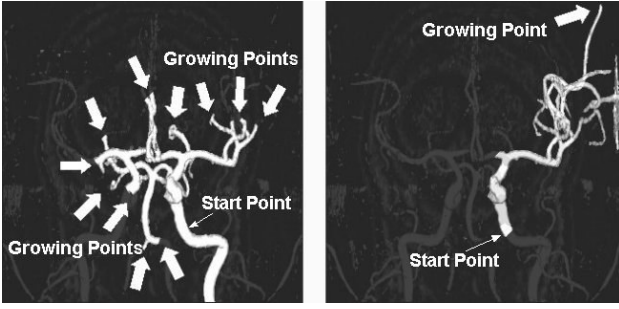


Figure 2. Comparison of region-growing method:
left: ordinary method, right: branch based method.

2.2 Branch based region-growing

The branch-based region growing performs the region-growing branch by branch and if growing point reaches a branch bifurcation part, let it go into only one side of the branches. Figure 3 shows an example of the growing at a branch bifurcation. The left figure shows the ordinary region growing and the right figure shows branch-based region growing. The number written in a voxel means the order of extraction step. When growing point reaches an edge of the vessel, the growing stops, and then, it starts again from the latest branch bifurcation point as shown in Figure 4.

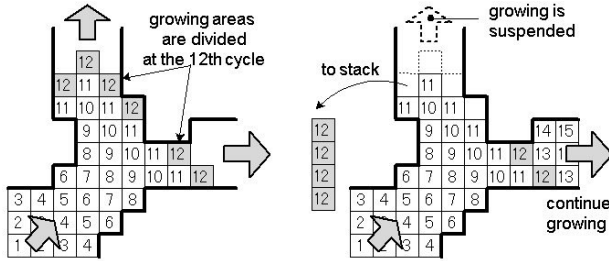


Figure 3. Processing of growing at the branch connection:
left: ordinary method, right: branch based method.

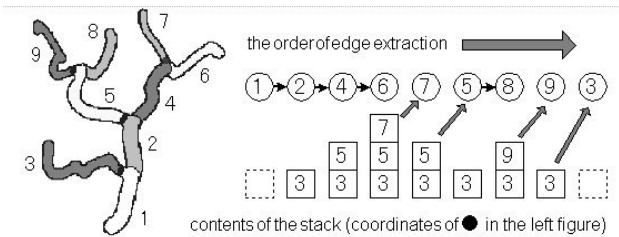


Figure 4. Order of the branch extraction and the contents of the stack.

2.3 Detection of branch bifurcation

In every growing cycle, the connectivity of the region added at the cycle is examined to find a branch bifurcation. This process is done as follows:

1. Start the region growing from one of the voxels in the added region. In this growing, the targets (voxels to be extracted as the connected object of added region) are the voxels which have the same cycle number.
2. After the growing finishes, voxels in a part of the added region are labelled as new parent voxels of the next cycle of branch-based region growing.
3. The voxels which are not connected are treated as the branch to be traced later.

To reduce over-dividing of branches, the region growing for checking connectivity are modified by the following modifications:

1. Use 26-neighbourhood to grow diagonal directions. (Original region growing uses 6-neighbourhood.)
2. Extend the range of the target cycle number of grouping to 2 from 1 as shown in Figure 5.

The number of branches detected according to the growing conditions described above is shown in Table 1.

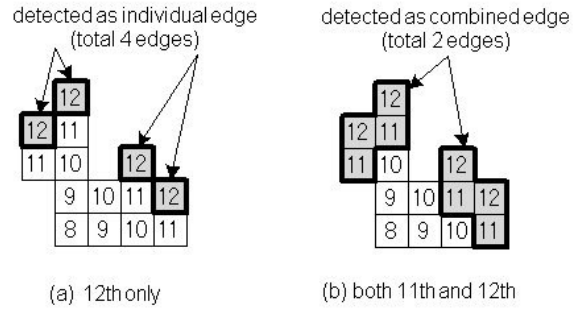


Figure 5. Voxels incorporated as connected region.

Growing condition		number of branches
thickness	neighbours	
1	6	96390
1	26	204
2	6	159
2	26	115

Table 1. Number of detected branches under several growing conditions.

2.4 Dynamical change of the growing conditions

Next step for the branch based region-growing is how to change the growing condition.

One of methods commonly used is to modify growing conditions according to the grey level intensity value of the area extracted recently. A typical example for this type of the growing condition is to use the following equation:

$$\mu - h\sigma \leq g(x, y, z) \quad (1)$$

where μ = average intensity of the neighbouring region during a certain duration of the resent growing steps.
 σ = intensity deviation of the same neighbouring region as the above defined.

$g(x,y,z)$ = the intensity value of the target voxel
 x,y,z = the coordinates of the target voxel
 h = a parameter which corresponds to control the easiness of growing.

The results obtained by the vessel segmentation using the above condition were not satisfactory ones in which many parts of shortages were found. The main reason of this seems to be that the intensity value changes widely in the vicinity of the branch bifurcation.

We carried out a branch-based region growing as a trial to check the actual intensity transition within blood vessels. The voxels with more than 70 intensity level (max=255) are set as the target voxels. Figure 6 shows the linkages between branches and branch attributes (length, thickness and intensity value). Each rectangle corresponds to each branch unit, i.e., region between bifurcations. The brightness inside rectangles indicates the intensity value of the corresponding branch unit, and its length and width indicate the length and thickness of the branch unit respectively.

This figure shows that the average values of the intensity and the thickness of the vessel widely change in the vicinity of the branch. The relation between the intensity and the thickness of each branch is shown in Figure 7. The horizontal axis indicates vessel thickness obtained by counting the number of voxels in the cross section area and the vertical axis indicates the average intensity of each branch unit.

We can see a close relation between the thickness and the intensity on this figure. Especially, in the range of section area (thickness) less than 30, this relation seems almost linear. On the other hand, there exist several dots which don't fit to the relation. They seem to correspond to the leak region. By getting rid of these dots on branch units, we can get more proper results. The following equation is proposed for this purpose:

$$\mu_i = \begin{cases} c_{\min} + kd_i & (d_i < d_c) \\ c_{\min} + kd_c & (d_i \geq d_c) \end{cases} \quad (2)$$

where μ_i = average intensity of i -th extracted branch
 d_i = average thickness of i -th extracted branch
 c_{\min} = lower limits of the intensity of ROI
 k = exclusive rate (if $k=0$, all branches are accepted)
 d_i = upper limits of the thickness range that the linear relation between thickness and intensity is formed.

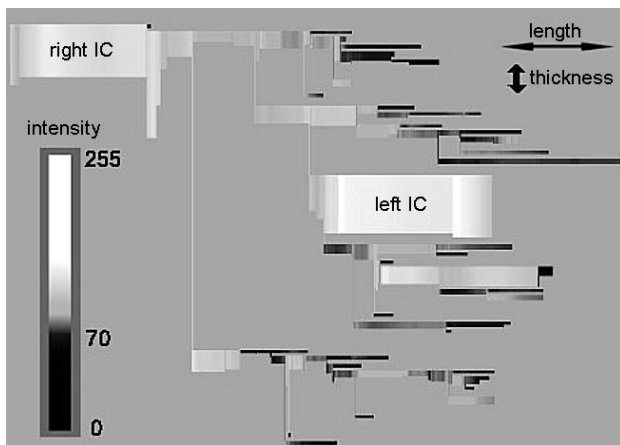


Figure 6. Attributes and linkages of extracted branches.

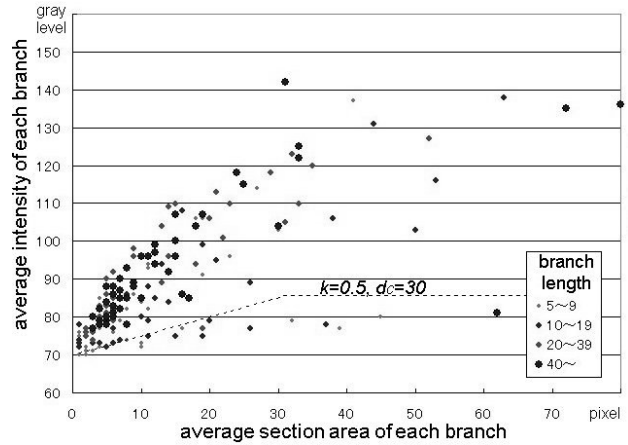


Figure 7. Relation between the thickness and the intensity of each branch unit.

2.5 Connection search over a gap

In the case of a narrow and long region like a blood vessel, a break of growing often occurs because of missing voxels on the way. This problem can be solved by extending the searching area for vessels. But it increases over-extraction errors and needs a lot of processing time.

In fact, the break occurs at the edge of the vessel, and it is enough to search for vessels at that point only. In the branch-based region growing, the growing stops at the each edge of the vessel, and then starts seeking vessels over a gap. If a vessel to be connected is found, the extracting process starts again, otherwise, the process enters into the next branch extraction.

Figure 8 shows results of segmentation. The start point of the region growing was set at a point inside the carotid artery. In the case of this data, as the intensity of a posterior communicating artery is partially low, the following vertebral artery and some subsequent vessels are not extracted by the conventional method shown in the left image. By using our method presented above, those vessels are extracted and moreover narrow vessels of parietal region are also detected as shown in the right image.

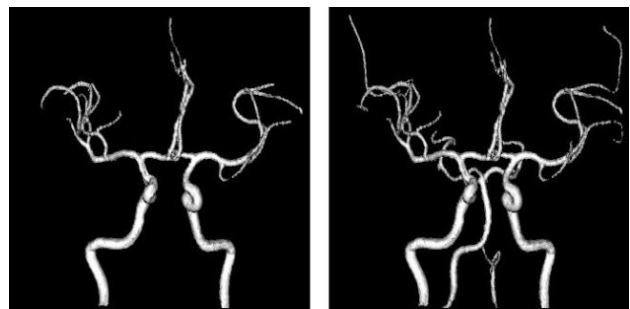


Figure 8. Effectiveness of the connection search: Left: not applied, Right: applied.

2.6 Evaluation of the Results

It is a difficult problem how to evaluate the results of segmentation. We can evaluate only subjectively the results by observing 3-D images of the extracted region. Moreover, as the shapes and location of blood vessels are not stable like brain or other organs, it is quite difficult to judge whether the results of detection are success or failure by observing 3-D images. Consequently, the objective evaluation method, in which the result is measured and shown by numeric value, is necessary for blood vessel segmentation.

Properly segmented 3-D reference data for the ordinal organs are obtainable by the manual segmentation on each slice data. In this case the numeric evaluation is possible by measuring the difference between the result of the segmentation and 3-D reference data. But in the case of blood vessels, manual segmentation is impossible because it is quite difficult to recognize blood vessels on MRA slice images correctly.

Here we propose a new evaluation method which compares two projection images. One is a group of 2-D vessel region images, which are manually extracted from MIP and used as reference data. Hereinafter we call it "segmented MIP" for short. It is easy to distinguish vessel region on MIP and 2-D manual segmentation can be performed without fail. The result of 3-D segmentation is also projected to the same directional plane as the MIP data. We call it projected result and it is used for the projection image for evaluation with segmented MIP.

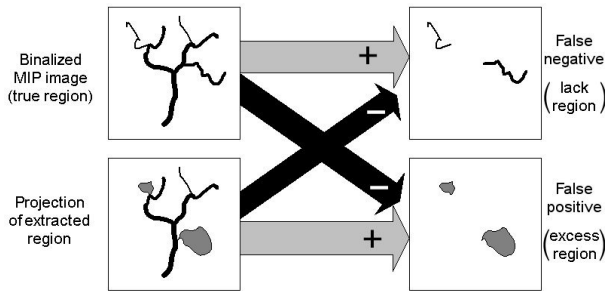


Figure 9. Evaluation method of segmentation.

The evaluation value is obtained by counting the number of the pixels on the image given by subtraction operation of two projection images mentioned above. More precisely, as shown in Figure 9, the shortage regions are acquired by subtracting projected result from segmented MIP. The excess regions are acquired by subtracting segmented MIP from projected result. Thus we can get false negative and false positive error index value, respectively.

In this evaluation process it may often happen that the thicknesses of vessels are different on two images and it causes erroneous edges of the vessels appear on the differential images. So, the vessels on the image going subtraction process are thinned previous to the subtraction so that the erroneous edges do not appear.

An example of differential images is shown in Figure 10. The black lines in the left image indicate the shortage region, and

those in the right indicate the excess region. Each image is obtained along x, y and z axis, and the sum of pixels on these three images is used as index values of the extraction error.

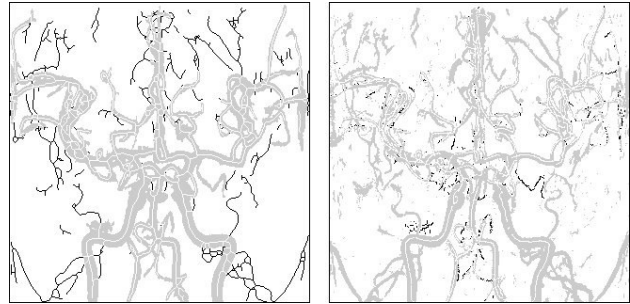


Figure 10. Differential image for evaluation.

left: pixels of shortage right: pixels of excess.

3. DISCUSSION

3.1 MRA data

We evaluate our segmentation method using 5 head MRA data obtained from 3 volunteers. Data-I is acquired from 1.5T MRI and the others are acquired from 3T MRI. Both MRI machines are manufactured by Siemens. Specifications of each data set are shown in Table 2. The data depth is 16 bits / voxel and 9-10 bits are effectively used. To reduce variation of intensity range between the data sets, the intensity values are normalized to 8bits / voxel.

Data	Person	Resolution	Slices
I	A	512 x 512	168
II	B	384 x 512	72
III	C	384 x 512	72
IV	B	288 x 384	128
V	C	288 x 384	128

Table 2. Specifications of MRA data sets

3.2 Experiment

We performed vessel region segmentation for each data set using the following methods.

- A) Normal (conventional) region growing
- B) Branch-based region growing:
 - with searching process at the edge of the branch
- C) Branch-based region growing
 - with searching process at the edge of the branch and removing non-vessel region

On each data, we set the starting point at the bottom of the left carotid artery. Growing condition c_{min} in eq.(2) is changed every 5 steps in the feasible range. In method-C, parameters are experimentally determined as $k=0.5$ and $d_c=20$. In method-A and method-B, parameters k, d_c are unused. ($k=d_c=0$)

The extraction error of data-I is shown in Figure 11. Each bar on the same growing condition corresponds to the method-A, -

B, -C respectively. The lower part of each bar (painted light grey) reveals the shortage error and the upper part (dark grey) reveals the excess error. As the tendency of every data was almost the same, hereinafter, we talk about the evaluation of data-I as the representative example.

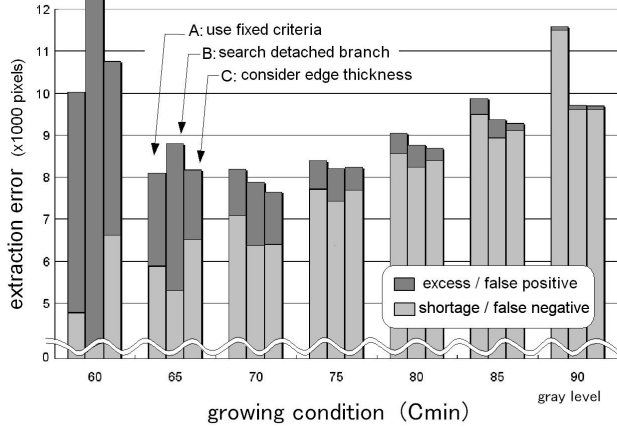


Figure 11. Extraction error of data I.

3.3 Shortage error (false negative)

The shortage error in all methods increases as c_{min} becomes large. The following differences are appeared among the three methods compared under the same c_{min} .

The shortage error in method-B is less than that of method-A for all c_{min} . The reason is that the vessels beyond the gap are connected and added to the extracted region in the method-B. Especially, improvement at $c_{min}=90$ is conspicuous, this is because of the addition of posterior communicating artery (already shown in Figure 8).

In method-C, as the region to be extracted is restricted based on the relation between the thickness and the intensity, the shortage error is a little bit larger than that of method-B. This tendency is more remarkable as c_{min} becomes smaller.

3.4 Excess error (false positive)

Excess error decreases as c_{min} becomes large in all methods. The tendency of the excess error in each method is as follows.

The excess error of method-B is larger than that of method-A under all conditions. This reason is that some connections to non-vessel region are added accidentally. On the other hand, the excess error of method-C is equal to or less than that of method-A. This reason is that most of the accidental connections were removed by the restriction based on the relation between thickness and intensity.

3.5 Total error of extraction

Total error is obtained by summing up the shortage error (false negative) and the excess error (false positive). As shown in Figure 10, both errors are countable as the number of pixels in line-shaped regions and the sum of the both error is treated as the error index which is shown as the height of bars in Figure 11.

The evaluation of each method is performed by comparing their total error on the same growing condition c_{min} . In practical use, as the c_{min} which produces minimum error is often used for segmentation, we made a comparative evaluation of their superiority under the optimized c_{min} .

As is clear from Figure 11, the optimized c_{min} of data-I is 70. As to other data (II, III, IV, V), 55,55,70,75 are obtained as the optimized c_{min} respectively. Total error of each method under its optimized c_{min} is shown in Figure 12. To help for comparison among three methods, the vertical axis in this chart represents the ratio of the total error to that of method-A.

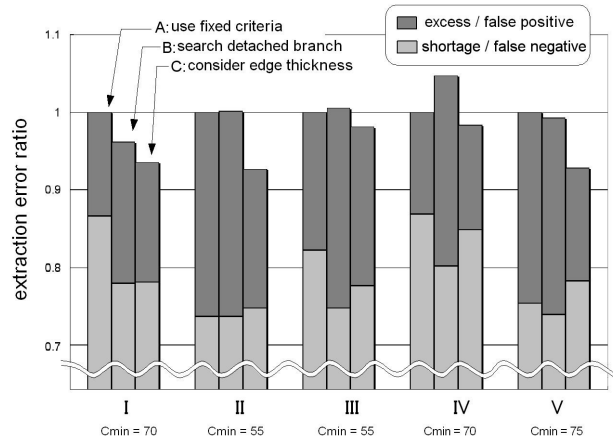


Figure 12. Extraction error ratio under optimized C_{min}

As a whole, the shortage error of method-B is smaller than that of method-A, but the excess error in method-B is always larger than that of method-A. Consequently, the total error of method-B is not always smaller than that of method-A. In these 5 data, the results are as follows: almost the same (within 1%): 3, improved: 1, deteriorate: 1. That is, the advantage of method-B against method-A is not recognized.

Method-C decreases the shortage error and increases the excess error as well as method-B. But the excess error of method-C is quite smaller than that of method-B. And so, the total error of method-C is always smaller than method-B and also smaller than method-A in most cases.

The deteriorate ratios of total error of method-C to that of method-A are 6.5, 7.4, 1.9, 1.7, 7.2[%]. These results lead us to the conclusion that our proposed method-C has a good effect on blood vessel segmentation for MRA data. Several 3-D images of the extracted vessel region obtained by method-C are shown in Figure 13 and 14.

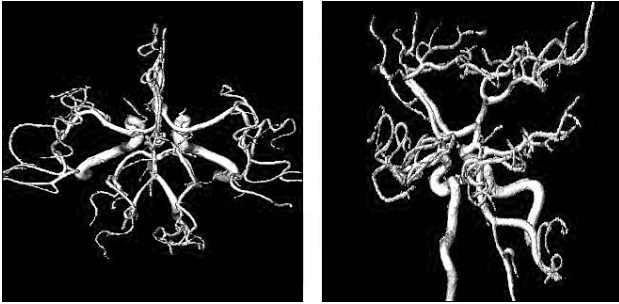


Figure 13. 3-D images of the extracted vessel (data-I)

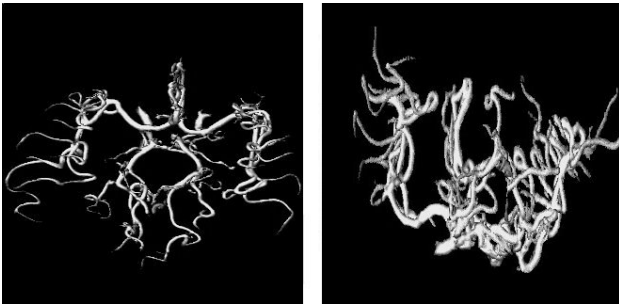


Figure 14. 3-D images of the extracted vessel (data-II)

4. CONCLUSIONS

We have developed a branch-based region growing algorithm which is designed for blood vessel segmentation for MRA data. We examined our segmentation algorithm and its appropriate growing conditions for this method. In addition, to perform an objective evaluation on the segmentation result, we developed the evaluation method based on projection images. We applied 5 MRA data sets to our segmentation method, and we confirmed the validity of our proposed method.

The biggest problem of our method is its processing time. It takes about 5 minutes to get one segmentation result, which is ten times longer than conventional region-growing method. Most of the time is consumed for branch bifurcation detection. It is necessary to optimize the processing for our method to be practical.

The growing condition we have shown is only one instance among many. Further discussion on the growing condition is still required to utilize this method effectively and to improve segmentation reliability.

Acknowledgements

This paper is supported in part by Informatics Research Centre for Development of Knowledge Society Infrastructure and also Intelligent Assistance in Diagnosis of Multi-dimensional Medical Images in Grant-in-Aid for Scientific Research on Priority Areas.

References

Masutani, Y., Masamune, K., Dohi, T., 1993. Region - growing based feature extraction algorithm for tree-like objects. *Proc. of VGC'96, Visualization in Biomedical Computing*, pp.161-167.

Masutani, Y., Schiemann, T., Hohne, K.H. 1998. Vascular shape segmentation and structure extraction using a shape-based region-growing model," *Proc. MICCAI'98*, pp.1242-1249.

Frangi, A.F., et.al., 2001. Quantitative Analysis of Vascular Morphology From 3D MR Angiograms: In Vitro and In Vivo Results," *Magnetic Resonance of Medicine* Vol.45, No.2, pp.311-322.

Fang, L., Wang, Y., Qiu, B., Qian, Y., 2002. Fast Maximum Intensity Projection Algorithm Using Shear Warp Factorization and Reduced Resampling," *Magnetic Resonance of Medicine* .47(4), pp.696-700.

Wilson, D.L., Noble, J.A., 1997. Segmentation of Cerebral Vessels and Aneurysms from MR Angiography Data, *Proc. of Information Processing in Medical Imaging*, pp.423-428.